St. Petersburg State University

Han Yunfei

On wavelet processing of numerical flows

Pre-graduate Practice

Report

Mathematical support and administration of information systems

Scientific supervisor:

professor

Burova I.G.(Бурова И.Г.)

Content

Abstract

In the field of Numerical Calculation, many problems can be transformed into the Fredholm integral equation. The recent appearance of wavelets as a new computational tool in applied mathematics has given a new direction to the area of the numerical solution of Fredholm integral equations. In this paper we will have a good understanding of the history of wavelets in chapter 1.we will discuss the Compression Algorithm using wavelets in chapter 2. In chapter 3 and 4 we will fully introduce how to construct the Haar wavelet and the Daubeshi wavelets. In the 5-th part we will conduct several methods using different wavelets to solve the Fredholm integral equation. we also have some numerical experiments and compare the results in the final chapter.

Problem statement

- To conduct a historical analysis of the origin and development of wavelets.

- Describe the applications of Haar wavelets, including image processing and compression.

- Consider the application of Haar wavelets to the solution of integral equations.
- Consider the application of Spline-wavelets of the zero degree to the solution of integral equations.

Introduction

Currently, when solving various problems of processing numerical streams, much attention is paid to wavelets. There are a large number of textbooks and manuals on the application of wavelets to solving various problems [1]-[50]. This is signal processing, this is image processing, this is the solution of integral equations. There are monographs by famous authors: Chuya, Daubechies. Interesting information about wavelets is given in the manual M.N. Yudin Yu.A. Farkov D.M. Filatov "Introduction to wavelet analysis"(М.Н. Юдин Ю.А. Фарков Д.М. Филатов «Введение в вейвлет-анализ»). Let's quote a few important and interesting fragments from this work.

The English term “wavelet” (fr. “ondelette”) literally means “a small wave. The author of the term “wavelet" is Jean Morlaix. He invented and applied his famous “Morlaix wavelet” in connection with the tasks of seismic exploration.

The term “splash” as an equivalent of the English “wavelet” was proposed to be used in 1991 by K. I. Oskolkov (К. И. Осколков).

The first wavelet were built by Haar in 1909. In 1910 Haar proposed the first wavelet canonical orthogonal group in $L_2(R)$, the orthogonal Haar group. The process of work is as follows. The orthogonal Haar basis is constructed using the transformation and decomposition of a binary function as a parent wavelet. Note that the advantages of the Haar wavelet transform include optimal resolution in the domain. There are some disadvantages: the Haar wavelet basis is not a continuous function, so the image resolution when using the Haar wavelet transform in the frequency domain is quite low. Let us mention some achievements in signal theory that came close to the design of bursts in the paper by E. I. Sakharova, A. A. Makashov, A. N. Kropotov "Using Haar wavelets for image processing and gluing" (Е. И. Сахарова, А. А. Макашов, А. Н. Кропотов «Использование вейвлетов Хаара для обработки и склейки изображений»). Haar splines were used for image processing.Fig. 1 shows Haar wavelets of the first level of decomposition.

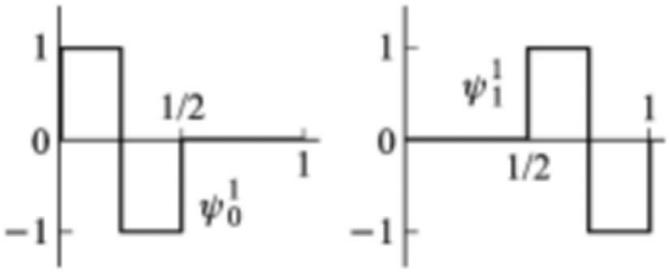

Fig.1. Haar wavelets of the first level of decomposition

With the help of the CRA in 1987, I. Daubechies constructed an infinite series of wavelets that possess the main property of the Haar system, namely orthogonality and a compact carrier. The works of V. L. Rvachev and V. A. Rvachev (В. Л. Рвачева и В. А. Рвачева) of 1971-1973 are directly related to the wavelets. These scientists have written out a wide class of differential equations with solutions with a compact carrier. As a special limiting case, it also included an equation that defines the Daubechies wavelets. The first articles by Russian authors on the theory of bursts were published in 1992. Several international conferences were held in the CIS (Moscow, 1995; Dnepropetrovsk, 1996; Dubna, 1998; St. Petersburg, 1999, Yekaterinburg, 2000, etc.), where various aspects of the theory of wavelet analysis were discussed among other problems of approximation theory.

Currently, many theorems about compression and recovery using wavelets are known. Restoring functions with a limited width .The Kotelnikov-Shannon theorem (теорема Котельникова-Шеннона) gives a Fourier spectrum over the values of the function for discrete values of the argument. The wavelet associated with this theory is called the Shannon wavelet. In 1946, D. Gabor proposed a generalization of the Fourier method, intermediate between the standard Fourier transform and wavelet analysis.

The mathematical system of axioms hidden behind the construction of wavelet analysis is currently called multiple-resolution (or multiple-scale) analysis (multiresolution analysis).

An explicit multiple-resolution analysis underlying the discrete wavelet transform was formulated in the fall of 1986 by S. Malla and I. Meyer. In 1936, Littlewood and Paley created the theory of grouping binary frequency components for Fourier series (that is, the $L-P$ theory: the phase of the Fourier transform grouped by binary frequency components does not affect the size and shape of the function), which is the earliest source of multiscale analysis of the idea.

From 1952 to 1962, Calderon and others extended $L-P$ theory to large dimensions and created the theory of singular integral operators.

In 1965, Calderon discovered the famous regeneration formula, which gave the atomic decomposition of H1 in parabolic space. In 1974, Koifman carried out the atomic decomposition of one-dimensional space and high-dimensional space. In 1976, using the theory for a uniform description of the Besov space, Pitre gave a set of bases of the Besov space. In 1981 Stromberg introduced the orthogonal basis of the Sobolev space, modified the orthogonal Haar basis and proved the existence of the wavelet function.

In 1981, the French geophysicist Morlaix proposed a formal concept of wavelets.

In 1985, the French mathematician Meyer proposed a condition for the admissibility of continuous wavelets and a formula for its recovery. In 1986, when Meyer proved that it is impossible to simultaneously have an orthogonal wavelet base having a certain regularity (i.e. smoothness) in the time-frequency domain, he accidentally discovered a smoothness function with a certain attenuation to construct a canonical orthogonal base (R) (i.e. Meyer base), thus proving the existence of an orthogonal wavelet- systems.

From 1984 to 1988, Meyer, Battle and Lemari, respectively, gave wavelet basis functions with fast attenuation characteristics: Meyer wavelet, Battle-Lemari spline wavelet.

In 1987 Mallat introduced the idea of multiscale analysis in the field of computer vision into wavelet analysis, proposed the concept of analysis with multiple resolutions, unified the structure of all previous specific orthogonal wavelets, gave a general method for constructing orthogonal wavelet bases and proposed a fast wavelet transform (that is, Mallat's algorithm).

In 1988, Daubechies constructed a smooth orthogonal wavelet basis (i.e., the Daubechy basis) with a finite set of branches based on the polynomial method.

Chinese scientist Wang Jianzhong and Chui constructed a single orthogonal wavelet function based on a spline function and proposed a general method for constructing a scale function and a wavelet function with optimal localization performance. In 1988, Daubechies spoke at a symposium on wavelets organized by NSF/CBMS in the United States, which attracted the attention of mathematicians, physicists, engineers and entrepreneurs and led the development and practical application of the theory of wavelets.

In 1992, Daubechies summarized and expanded the content of these lectures, published a classic work in the field of wavelets - "Ten Lectures on Wavelets".

In March 1992, the international authoritative journal “IEEE Transactions on Information Theory” published a special issue "Wavelet analysis and its application", which comprehensively presents the previous theory and application of wavelet analysis and its development in various subject areas. Since then, the wavelet analysis has entered the stage of comprehensive application. In 1992, Kovacevich and Vetterli proposed the concept of biorthogonal wavelets.

In 1992, Cohen, Daubechies, and Fauve constructed biorthogonal wavelets with properties such as symmetry, tight support, vanishing moment, and regularity.

In 1992, Koifman and Vikerhauser proposed wavelet packet analysis (WP).

In 1992, Zou et al. proposed the theory of multiband wavelet (M-band Wavelet), which expanded people's research on wavelet transformation from "dual-band" situations to "multiband".

In a multi-resolution analysis based on a "two-band" wavelet transform, the scale function corresponds to a low-pass filter, while the wavelet function corresponds to a high-pass filter. The "dual-band" wavelet transform decomposes the signal into different channels, and the bandwidth of these channels is the same relative to the logarithm of the scale function, so high-frequency channels have a wide bandwidth, while low-frequency channels have a narrow bandwidth.

In 1993, Goodman et al. created a theoretical structure with multiple wavelets based on multiscale r-order functions and multi-resolution analysis.

In 1994, Geronimo et al. proposed the multi-wave transform (MWT), which extended the single-scale wavelet transform to the multiscale wavelet transform.

In 1991, Alpert used polynomials to construct the first multi-wavelet. Geronimo et al. used the fractal interpolation function to construct an orthogonal, symmetric, rigidly supported and approximating multi-wavelet GHM of order 2.

In 1995, Sveldens (Свельденс) et al. proposed a new algorithm for constructing wavelets. This marks the beginning of the second generation of wavelets.

2 The compression algorithm using wavelets

Wavelet decomposition is widely used in image compression. In applications, an uncompressed two-dimensional array has a very large size, and it requires high speed and a lot of memory to restore. In the process of processing large amounts of data or large volumes of images, or obtaining large-sized images, there may be a shortage of resources (for example, memory). To speed up the process of building video, compression of incoming video information is often used. Therefore, it is necessary to choose the appropriate compression and decompression algorithm.

The purpose of the algorithms is to transform the image so that it is well compressed by classical algorithms. It is clear that long sequences of zeros are best compressed. To write 1000 zeros to memory, you can simply write the number 1000 (with a note that this is the number of zeros). Next, a decoding program works, which recognizes that zeros were meant and prints them. However, if there is suddenly one in the middle of the sequence of zeros, then it is not enough to set only the number 1000 (zeros). If we look at the photo, it is clear that slight fluctuations in brightness are invisible. Therefore, when encoding, you can change the image so that the compression ratio will immediately increase. At the same time, the errors introduced will be insignificant, since photos usually have such a feature: the brightness of neighboring pixels differs by a small amount, and contrast differences occupy only a small part of the image.

Consider the first 2000 pairs of neighboring pixels and represent each pair on the graph as a point. In almost all real images, the dots line up along one straight line. The upper left and lower right corners of the image are almost always empty.

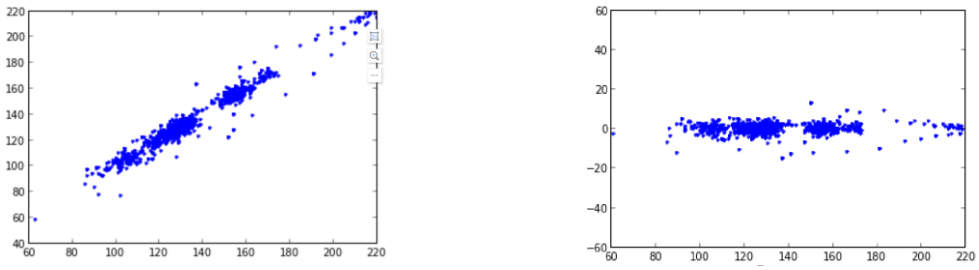

Fig.2. The previous scatter chart that has not been compressed (the left figure) and the scatter plot after being compressed(the right figure)

And now let's look at the right part of Fig. 2, the points in which will be half-sums and half-differences. The half-differences are in a narrower range of values.

The drawings from the dots on the two figures are the same. The difference is only in turning at an angle of 45 °. That is, the Haar transformation is simply an affine transformation — the rotation of points in such a way that they can be conveniently and compactly encoded.

Let us be given the color intensities of the image in the first row of the intensity matrix. Take, for example, such, 254, 255, 256, 257, 257, 257, 258, 256. It can be seen that the neighboring numbers are quite close. To do this, we divide all the numbers into pairs and find half-sums and half-differences of values in each of them:

(254, 255), (256, 257), (257, 257), (258, 256).

These arrays can be transformed into the form of a "half-sum" of the average value of *a* and a "half-difference" of the average difference of *d*, namely:

$(a, d) =$ (254.5, 0.5), (256.5, 0.5), (257, 0.0), (257, -1.0).

Note: the first value in the pair = *a* - *d*, the second value in the pair = *a* + *d*.

The resulting numbers can be rearranged by separating half-sums and half-differences:254.5, 256.5, 257, 257; 0.5, 0.5, 0.0, -1.0.

The numbers in the second half of the sequence will usually be small. In real images, neighboring pixels rarely differ significantly from each other. If the value of one is large, then the other is large, i.e. the pixels are correlated.

"half—sums" are the average values in pairs of pixels. That is, the values of "half—sum" are a reduced copy of the original image. Reduced because the "half-sum" is two times smaller than the original pixels. Half-sums average brightness values, that is, they "filter out" random bursts of values. We can assume that this is some kind of frequency filter. Similarly, the differences "distinguish" inter-pixel "bursts" among the values and eliminate the constant component. That is, they "filter out" low frequencies.

2.1 Compression Algorithm Decoding

Let's take a closer look at Compression Algorithm Decoding matrix.

$$\boldsymbol{H} = \begin{pmatrix} \frac{\sqrt{2}}{2} & \frac{\sqrt{2}}{2} \\ -\frac{\sqrt{2}}{2} & \frac{\sqrt{2}}{2} \end{pmatrix};$$

It consists of two vector strings: $\left(\frac{\sqrt{2}}{2} \quad \frac{\sqrt{2}}{2}\right)and\left(-\frac{\sqrt{2}}{2} \quad \frac{\sqrt{2}}{2}\right)$, Let's call them $\boldsymbol{v_1}$ and $\boldsymbol{v_2}$.

These vector strings have the following properties:

1. Their lengths are equal to 1, that is $\boldsymbol{v_1 v_1{}^T = v_2 v_2{}^T = 1}$;

Note: multiplying a vector string by a transposed vector string is a scalar product.

2. they are orthogonal, that is$\boldsymbol{v_1 v_2{}^T = v_2 v_1{}^T = 0}$;

the matrix is a pair of scalars or vectors that need to be connected. Such a transformation is described by the matrices *H*:

$$\boldsymbol{H} = \begin{pmatrix} \frac{1}{2} & \frac{1}{2} \\ -\frac{1}{2} & \frac{1}{2} \end{pmatrix} = \frac{1}{2} * \frac{1}{2} - (-\frac{1}{2}) * \frac{1}{2} = \frac{1}{2};$$

2.2 Normalization

With affine transformations, the area of the figure may change. The area change coefficient is equal to the determinant of the matrix. In order for the determinant to become equal to one, it is necessary to multiply each element of the matrix by $\sqrt{2}$.

$$H = det \begin{pmatrix} \frac{\sqrt{2}}{2} & \frac{\sqrt{2}}{2} \\ -\frac{\sqrt{2}}{2} & \frac{\sqrt{2}}{2} \end{pmatrix} = 1;$$

On the angle of rotation (and hence on the "compressive capacity" of the transformation) it won't affect. In order to apply the transformation to the entire image we can describe the transformation with a matrix, but larger in size. The diagonal of this matrix will consist of the matrices *H*:

$$H = \begin{pmatrix} \frac{\sqrt{2}}{2} & \frac{\sqrt{2}}{2} & & \\ -\frac{\sqrt{2}}{2} & \frac{\sqrt{2}}{2} & & \\ & & \frac{\sqrt{2}}{2} & \frac{\sqrt{2}}{2} \\ & & -\frac{\sqrt{2}}{2} & \frac{\sqrt{2}}{2} \end{pmatrix} \ddots;$$

2.3 Inverse transformation

As we know, if the determinant of a matrix is not zero, then there is an inverse matrix for it that "cancels" its action. If we find the inverse matrix for *H*, then decoding will consist simply in multiplying vectors with half-sums and half-differences by it.

$$H^{-1} = H^T = \begin{pmatrix} \frac{\sqrt{2}}{2} & \frac{\sqrt{2}}{2} \\ -\frac{\sqrt{2}}{2} & \frac{\sqrt{2}}{2} \end{pmatrix}^T = \begin{pmatrix} \frac{\sqrt{2}}{2} & -\frac{\sqrt{2}}{2} \\ \frac{\sqrt{2}}{2} & \frac{\sqrt{2}}{2} \end{pmatrix};$$

"half—sums" are the average values in pairs of pixels. That is, the values of "half—sum" are a reduced copy of the original image. Reduced because the "half-sum" is two times smaller than the original pixels. Half-sums average brightness values, that is, they "filter out" random bursts of values. We can assume that this is some kind of frequency filter. Similarly, the differences "distinguish" inter-pixel "bursts" among the values and eliminate the constant component. That is, they "filter out" low frequencies.

---

3 Haar Wavelets

As mentioned earlier, the Haar Wavelet is one of the first constructed and simplest wavelets. It is based on the construction of an orthogonal system of functions proposed by the Hungarian mathematician Alfred Haar in 1909. Thus, Haar wavelets are orthogonal, have a compact carrier, are well localized in space, but are not continuous and are not smooth.

3.1 Building a Haar wavelet

The parent (mother) wavelet function $\psi(x)$ with the zero value of the integral $\int_{-\infty}^{+\infty} \psi(x)dx = 0$, which determines the details of the signal, is given as follows:

$$\psi(x) = \begin{cases} 1, & 0 \le x < 1/2 \\ -1, & 1/2 \le x < 1 \\ 0, & x \notin [0,1) \end{cases}$$

The scaling function $\varphi(x)$ with a unit integral value $\int_{-\infty}^{+\infty} \varphi(x)dx = 1$ that determines the rough approximation of the signal is constant:

$$\varphi(x) = \begin{cases} 1, 0 \le x < 1 \\ 0, x \notin [0,1) \end{cases}$$

3.2 Haar transformation

Let the numerical stream in question encode some image displayed on the computer screen. Suppose that the screen is a rectangular matrix of a large number of pixels - small rectangles applied to a transparent surface (glass) that glow under the influence of electrons falling on them, and for such a glow there is a fixed number of brightness gradations. For simplicity, we consider only monochrome images (black and white screen).

Usually the pixels are numbered sequentially in rows, which are pre-arranged one after the other in a straight line; thus, the pixels acquire numbers

$$0, 1, 2, \ldots, N - 1, where\ N = M \times K,$$

where *M* is the number of rows of the matrix under consideration, and *K* is the number of its columns. For certainty, we will assume *N* to be even; let *N = 2L*, where *L* is a natural number. Each pixel is assigned a certain brightness, expressed by a certain number; let's denote this number for the jth pixel by $\mathbf{c_j}$. Thus, the encoding of the image is performed using a numeric stream

$$\mathbf{c_0},\ \mathbf{c_1},\ \mathbf{c_2}\ \ \mathbf{c_3}, \mathbf{c_4},\ \mathbf{c_{2L-1}}. (3.1)$$

The stream (3.1) can be transmitted over communication lines and, when fed to a computer (TV) screen, can be turned into the original image. If the original image is transmitted with great accuracy, then N is large, and the transmission of even one such image presents significant technical difficulties (in practice, it is required to transmit millions of such images at high speed). Therefore, the problem arises of reducing the number of transmitted numbers. Assuming that the neighboring numbers in (3.1) are close, one could suggest transmitting, for example, only numbers with odd numbers in (3.1), i.e. numbers:

$$\mathbf{c_1, c_3, c_5, c_7, \ldots, c_{2L-1}} \quad (3.2)$$

Such a transformation is called thinning of the original numerical stream (the English term upsampling is rarefaction or sparse sampling). Instead of the stream (3.1), a twice shorter stream (3.2) is transmitted; the receiving device expands the received numerical stream (3.2) by duplicating the received values so that, as a result, the same numbers are found in places with an even and the next odd number. As a result, an image obtained using a numerical stream of the form of a number is reproduced on the screen:

$$\mathbf{c_1,\ c_1,\ c_3,\ c_3, c_5, c_5, c_7\ c_7, \ldots, c_{2L-1}, c_{2L-1}} \quad (3.3)$$

Thus, the "restoration" (3.3) of the original stream (3.1) is performed with an error, and the information is lost irreversibly (i.e., without transmitting additional information, the receiving device, generally speaking, is not able to restore the stream (3.1)). Such a technique (the English equivalent of downsampling – thickening) is justified if the resulting image differs little from the original one.

The disadvantages of the described approach are as follows:

1) it is applicable only to a rather slowly changing flow,

2) there is no consideration of the characteristics of the numerical flow (in some parts, the numerical flow can change very slowly, and it would be possible to

throw out many numbers in a row, and in other parts, with a rapid change in the flow, any number ejections can significantly spoil the transmitted image),

3) there are no means to clarify the transmitted stream.

The idea of the wavelet approach is illustrated as follows. Two numerical streams are formed from the numerical stream (3.1)

$$a_j = (c_{2j} + c_{2j+1})/2\,; b_j = (c_{2j} - c_{2j+1})/2\,; where\ j = 0, 1, 2, \ldots, L\ -\ 1. \quad (3.4)$$

It is not difficult to see that

$$c_{2j} = a_j + b_j; c_{2j+1} = a_j - b_j;\ j = 0, 1, 2, \ldots, L\ -\ 1. \quad (3.5)$$

Thus, if the stream (3.1) is replaced by two streams (3.4), then after their transmission, it is possible to restore the original stream (3.1) using formulas (3.5)

The question arises, what is the benefit of replacing the stream (3.1) with two streams (3.4), if the total number of numbers in the streams (3.4) coincides with the number of numbers in (3.1). To answer this question, note that if the neighboring numbers in (3.1) are close, then the second of the streams in (2.4) consists of numbers close to zero, so it may turn out that the second stream is not needed at all and can be discarded. However, if some fragments of the first stream from (3.4) do not give sufficient accuracy, then we can use the corresponding fragments (with the same index ranges) of the second stream, and make calculations using the formulas (3.5); this will lead to an accurate restoration of the original stream (3.1) in the relevant sections (a similar transmission technology is used, in particular, when transmitting images on the Internet: first, the main contours of the image appear, allowing us to evaluate its content and interrupt the transmission if it is not necessary, and only then there is a clarification and final completion image transmission).

We set a stream of numbers

$$\boldsymbol{a_0},\ \boldsymbol{a_1},\ \boldsymbol{a_2}, \boldsymbol{a_3}, \boldsymbol{a_4},\ \boldsymbol{a_{2L-1}}. \quad (3.6)$$

Which is called “the main wave” and another stream of numbers

$$\boldsymbol{b_0,\ b_1,\ b_2,\ b_3, b_4,\ b_{2L-1}}. \tag{3.7}$$

As a wavelet (burst) flow.

The resulting main stream (3.6) can be considered as compression of the original stream (3.1), and the stream (3.7) as an amendment to the main stream, allowing to restore the original stream.

Thus, the Haar transform is a pair of filters that divide the signal into low—frequency and high-frequency components. To get the original signal, you just need to combine these components again.

The theory of the algorithm for wavelet-compressed Haar images looks like this： The low-frequency component carries information about the general shape of the face, about smooth changes in brightness. High—frequency is noise and small details. When compressing, some of the high-frequency data can be discarded. Moreover, as we found out, it usually has smaller values, which means it is encoded more compactly. The compression ratio can be increased by applying the Haar transform repeatedly. After repeated application, high-frequency information will occupy 75%.

The black areas correspond to low brightness, that is, values close to zero:

1.They can be encoded with greater efficiency.

2. They can be reset to zero.

The JPEG compression algorithm implements a similar approach, only instead of the Haar transform, a discrete cosine transform is used.By changing the number of zeroing coefficients, you can adjust the compression ratio.

Obviously, when the image contains long segments with the same brightness value, the Haar transform will give the best results. Thus, the Haar transformation eliminates the constant component.

4 The Daubeshi Wavelet

In view of the situation when there are not so many areas of the same brightness in a real photo and linear variables need to be zeroed, the Belgian physicist and mathematician Ingrid Daubeshi proposed a wavelet function with hierarchical properties and named the wavelet after her name. Daubeshi is also one of the creators of the wavelet theory. Daubeshi wavelets are mainly used in discrete wavelet transformation. They are the most commonly used wavelet transform. They are commonly used in digital signal analysis, signal compression, and noise removal.

In general, discrete wavelet transformations are usually based on orthogonal wavelets, and Daubeshi wavelets are also orthogonal wavelets. Because it is easy to implement using fast wavelet transform (FWT).For finite-length wavelets, when applied to the fast wavelet transform (FWT), there will be two rows of real numbers: one is the coefficient of a high-pass filter called a wavelet filter (a wavelet filter, also known as a mother wavelet); the second is the low-pass filter coefficient.a transmission filter called a scaling filter (also known as father wavelet).

4.1 Classification of Daubeshi wavelets

The classification of Daubeshi wavelets is based on the value A of the vanishing moment (also the vanishing momentum number) (A is called tap). The smoothness of the scaling function and the wavelet function will increase as the value of the vanishing pulse (tap) increases: for example, when A=1, the Daubeshi wavelet is a Haar wavelet, and the correction function and the wavelet function are discontinuous. When A = 2, the correction function and the Daubeshi wavelet function are continuous functions that cannot be smoothly differentiated; when A = 3, the correction function and the wavelet function are already continuous and differentiable functions.

We use the length N of the filter to describe the filter as DN. For example, a Dobezi wavelet with N = 2 is written as D2, a Daubeshi wavelet with N = 4 is written as D4,

and so on (N is an even number).In fact, the commonly used Daubeshi wavelets have sizes from D2 to D20.Another relevant way to describe it is db N, where N refers to the number of moments of disappearance. Thus, D4 and db2 are the same Daubeshi wavelet.

Due to the complexity of Haar wavelets, when zeroing linear variables, the Daubeshi transform of the improved transformation will have more than two points. Hence, four values will be used for each value, and two will be moved each time.

That is, if the original sequence — $\mathbf{1}, \mathbf{2}, \mathbf{3}, \mathbf{4}, \mathbf{5}, \mathbf{6}, \ldots, \boldsymbol{N-1}, \boldsymbol{N}$, then we will take a four-seater$(\mathbf{1}, \mathbf{2}, \mathbf{3}, \mathbf{4})$, $(\mathbf{3}, \mathbf{4}, \mathbf{5}, \mathbf{6})$ etc. The last four "bites the sequence by the tail": $(\boldsymbol{N-1}, \boldsymbol{N}, \mathbf{1}, \mathbf{2})$.

In the same way, try to create two filters: high-frequency and low-frequency.Replace each four with two digits.Since the values of the quadratures overlap, the number of values will not change after the transformation.

In order to make it convenient to count the inverse matrix, we also require orthogonality of the transformation. Then the search for the inverse matrix is reduced to transposition.Let the brightness values in the four be equal . Then we will write the first filter in the form:

$$\boldsymbol{a = c_1 x + c_2 y + c_3 z + c_4 t};$$

The four coefficients forming the vector-row of the transformation matrix are still unknown to us.In order for the vector-string of coefficients of the second filter to be orthogonal to the first one, we take the same coefficients but rearrange them and change the signs:

$$\boldsymbol{d = c_4 x - c_3 y + c_2 z - c_1 t};$$

The transformation matrix will have the form:

$$\begin{pmatrix} c_1 & c_2 & c_3 & c_4 & & & & \\ c_4 & -c_3 & c_2 & -c_1 & & & & \\ & & & & c_1 & c_2 & c_3 & c_4 \\ & & & & c_4 & -c_3 & c_2 & -c_1 \\ & & & & & & & \ddots \end{pmatrix}$$

The orthogonality requirement is met for the first and second rows automatically. We will require that lines 1 and 3 are also orthogonal:

$$c_3c_1 + c_4c_2 = 0;$$

• Vectors must have unit length (otherwise the determinant will not be single):

$$c_1^2 + c_2^2 + c_3^2 + c_4^2 = 1;$$

• The transformation should reset the chain of identical values (for example, (1, 1, 1, 1)):

$$1c_4 - 1c_3 + 1c_2 - 1c_1 = 0;$$

• The transformation should reset the chain of linearly growing values (for example, (1, 2, 3, 4)):

$$1c_4 - 2c_3 + 3c_2 - 4c_1 = 0;$$

We obtained 4 equations connecting the coefficients. Solving them, we get:

$$c_1 = \frac{1+\sqrt{3}}{4\sqrt{2}}, c_2 = \frac{3+\sqrt{3}}{4\sqrt{2}}, c_3 = \frac{3-\sqrt{3}}{4\sqrt{2}}, c_4 = \frac{1-\sqrt{3}}{4\sqrt{2}}.$$

Substituting them into the matrix, we get the desired

transformation. After applying it to photos, we will get more zeros and small coefficients, which will allow us to compress the image more. This transformation is called a Daubeshi wavelet D4.

5 Integral equation

There are many applications of wavelet decomposition, and wavelet decomposition has broad prospects for application in numerical calculations.

5.1 The solution of the Fredholm integral equation of the 2nd kind on the use of Haar wavelets

.We will construct a calculation scheme, conduct numerical experiments on the use of wavelets (Haar wavelets) as a basic function, and solve the Fredholm integral equation of the second type using collocation.

$$x(t) - \lambda \int_A^B K(t,\tau)x(\tau)\,d\tau = f(t), t \in (A,B).$$

Basic concepts and definitions of the wavelet transform All Haar wavelets are a family of these basic function:

$$\psi_{ab} = \frac{1}{\sqrt{a}}\psi(\frac{t-a}{b})$$

it is obtained from a single function $\psi(t)$, called the mother wavelet, by means of its time shifts (b) and extensions (scaling) along the time axis (a). The multiplier$1/\sqrt{a}$

guarantees the independence of the norm of these functions from the scaling parameter a.

The wavelet transform of a signal is its representation in the form of a generalized series or Fourier integral over a system of basis functions. In this paper, the solution of the integral equation is carried out numerically, i.e. some discretization is carried out, so we will be interested only in the discrete wavelet transform. In addition, it requires less computing costs. The discretization is more convenient to perform through powers of two, namely: $a = 2^m, b = k * 2^m, m, k \in Z$;

With this in mind, the ratio will take the form

$$\psi_{mk} = \frac{1}{\sqrt{2^m}}\psi\left(\frac{t-2^m}{k*2^m}\right) = \frac{1}{\sqrt{2^m}}\psi(2^{-m} * t - k).$$

where *m* is called the scale parameter; *k* is the magnitude of the shift.

Thus, the forward and inverse dyadic wavelet transformations of the continuous function $f(t)$ will take the form, respectively

$$\boldsymbol{c_{mk} = \langle f(t), \psi_{mk}(t) \rangle = \int_{-\infty}^{\infty} f(t)\psi_{mk}(t)dt}$$

$$\boldsymbol{f(t) = \sum_{m.k} c_{mk}\psi_{mk}(t)}$$

$\langle \blacksquare, \blacksquare \rangle$, is the sign of the scalar product in space $L_2(R)$.

Remark. It should be noted that this is not yet a discrete transformation, since the function *f(t)* is continuous. In addition, the formulas for the wavelet transform of discrete signals cannot be obtained by simply sampling the formulas of the dyadic wavelet transform for a continuous signal.

To overcome these difficulties, as a rule, they switch to large-scale analysis, the essence of which is that when studying functions *f (t)*, it is convenient to represent them as a sum approximating (rough) and the detailing (refined) component

$$\boldsymbol{f\ (t) = A_m(t) + \sum_{j=1}^{m} D_j(t).}$$

with their further detailing by the iterative method.

Let there be a continuous function (signal)$\boldsymbol{f\ (t) \in V_0}$. We interpret the discrete signal as a sequence of coefficients ak obtained with scaling functions$\boldsymbol{\varphi_{ok}(t)}$ (also called paternal wavelets):

$$\boldsymbol{f\ (t) = A_0(t) = \sum_{k} a_{ok}\varphi_{ok}(t),}$$

where $\boldsymbol{a_{ok} = a_k(t) = \langle f\ (t), \varphi_{ok} \rangle;}$

a_{ok}----approximation coefficients at the level *m = 0* . According to the theory of large-scale analysis, the function f(t) is decomposed into two components belonging to subspaces V_1 and W_1, and $V_0 = V_1 \oplus W_1$:

$$f(t) = A_1(t) + D_1(t) = \sum_k a_{1k}\varphi_{1k}(t) + \sum_k d_{1k}\psi_{1k}(t).$$

where the new sequences$\mathbf{a_{ok}}$ and $\mathbf{d_{1k}}$ have half the length compared to $\mathbf{a_{ok}}$. Further, the decomposition process can be continued by$\mathbf{A_1(t)}$ (subspaces $\mathbf{V_2}$ and $\mathbf{W_2}$, where $\mathbf{V_1 = V_2 \oplus W_2}$). At the decomposition level m of the function $f(t)$ we obtain, respectively

$$f(t) = A_m(t) + D_m(t) + \cdots + D_1(t).$$

at the same time:

$$f(t) = \sum_k a_{mk}\varphi_{mk}(t) + \sum_{j=1}^{m}\sum_k d_{jk}\psi_{jk}(t);$$

Thus, at the minimum value of the scale m=0, the discrete sequence of its values fi (i=0, 1,...,N-1) of the function f (t) is taken as approximating coefficients, i.e. =f i (i=0, 1,...,N-1). The maximum value of the scale m is equal to and is determined by the number of samples of the signal (the number of samples is equal to $\mathbf{2^{n_0}}$). The value of k for the current m varies in the range from zero to $\mathbf{2^{n_0-m}-1}$.

5.1.1 Computational scheme

Consider the Fredholm integral equation of the second kind and fix some natural value $\mathbf{n_0}$. For the segment [A,B], we perform the partition

$$\mathbf{A = t_o < t_o < \cdots < t_o = B}$$

For the segment [A,B], we perform the partition in a constant step.

As the parent wavelet, we choose the Haar wavelet and the corresponding scaling function:$h = (B - A/N), where\ N = 2^{n_0}$;

As the parent wavelet, we choose the Haar wavelet $\boldsymbol{\varphi(t)}$ and the corresponding scaling function $\boldsymbol{\psi(t)}$ *:*

$$\boldsymbol{\psi(x)} = \begin{cases} \mathbf{1},\ \mathbf{0} \le \boldsymbol{x} < \mathbf{1/2} \\ -\mathbf{1},\ \mathbf{1/2} \le \boldsymbol{x} < \mathbf{1} \\ \mathbf{0}, \boldsymbol{x} \notin [\mathbf{0}, \mathbf{1}) \end{cases}$$

$$\boldsymbol{\varphi(x)} = \begin{cases} \mathbf{1}, \mathbf{0} \le \boldsymbol{x} < \mathbf{1} \\ \mathbf{0}, \boldsymbol{x} \notin [\mathbf{0}, \mathbf{1}) \end{cases}$$

The family of basic wavelets $\boldsymbol{\varphi_{mk}(t)}$and the corresponding scaling functions$\boldsymbol{\psi_{mk}(t)}$ is defined in such a way that the wavelets at the minimum value of the scale m = 0 along the length of the carrier occupy a segment : $\Delta_{\boldsymbol{k}} = [\boldsymbol{t_k}, \boldsymbol{t_{k+1}}], \boldsymbol{k} = \mathbf{0}, \mathbf{1}, \cdots, \boldsymbol{N} - \mathbf{1}$*:*

$$\boldsymbol{\psi_{mk}} = \frac{\mathbf{1}}{\sqrt{\mathbf{2^m}}} \boldsymbol{\psi}\left(\mathbf{2^{-m}} * \frac{(\boldsymbol{t} - \boldsymbol{a})}{\boldsymbol{h}} - \boldsymbol{k}\right),$$

$$\boldsymbol{\varphi_{mk}} = \frac{\mathbf{1}}{\sqrt{\mathbf{2^m}}} \boldsymbol{\varphi}\left(\mathbf{2^{-m}} * \frac{(\boldsymbol{t} - \boldsymbol{a})}{\boldsymbol{h}} - \boldsymbol{k}\right);$$

Where m= 0,1,...,, and the value of the parameter k for the current m varies in the range from zero to $\mathbf{2^{n_0 - m} - 1}$.

After the system of orthogonal functions $\boldsymbol{\psi_{mk}(t)}$ and $\boldsymbol{\varphi_{mk}(t)}$ are constructed, we determine the current value of the scale m equal to some fixed value *M (0 <M <=*$\boldsymbol{n_0}$*)* and we will look for a solution to the equation in the form

$$\boldsymbol{x^*(t)} = \sum_{\boldsymbol{k=0}}^{\mathbf{2^{n_0 - m} - 1}} \boldsymbol{a_{mk}} \boldsymbol{\varphi_{mk}(t)} + \sum_{\boldsymbol{j=1}}^{\boldsymbol{M}} \sum_{\boldsymbol{k=0}}^{\mathbf{2^{n_0 - j} - 1}} \boldsymbol{d_{jk}} \boldsymbol{\psi_{jk}(t)}$$

Substituting the ratio into the equation , we have:

$$\boldsymbol{A} = \sum_{\boldsymbol{k=0}}^{\mathbf{2^{n_0 - m} - 1}} \boldsymbol{a_{mk}} \left[\boldsymbol{\varphi_{mk}(t)} - \boldsymbol{\lambda} \int_{\boldsymbol{A}}^{\boldsymbol{B}} \boldsymbol{K(t, \tau)} \boldsymbol{\varphi_{Mk}(\tau)} \boldsymbol{d\tau} \right]$$

$$\boldsymbol{B} = \sum_{\boldsymbol{j=1}}^{\boldsymbol{M}} \sum_{\boldsymbol{k=0}}^{\mathbf{2^{n_0 - j} - 1}} \boldsymbol{d_{jk}} \left[\boldsymbol{\psi_{jk}(t)} - \boldsymbol{\lambda} \int_{\boldsymbol{A}}^{\boldsymbol{B}} \boldsymbol{K(t, \tau)} \boldsymbol{\psi_{jk}(\tau)} \boldsymbol{d\tau} \right]$$

$$A + B = f\ (t);$$

The basic wavelet$\psi_{jk}(t)$ constructed according to the relation (and similarly the scaling function$\varphi_{mk}(t)$), for fixed m, k is nonzero on the segment $[A + h * 2^m * k, A + h * 2^m * (k+1)], m = 1, 2 \ldots n_0, k = 0, 1, \cdots, 2^{n_0 - m} - 1$;

which also simplifies the relationship Further define the collocation points $\bar{t}_1$ as the midpoints of the segments$\Delta_i = [t_i, t_{i+1}]$,*i=0, 1,..., n-1*;

and we get the final approximating SLA:

$$A = \sum_{k=0}^{2^{n_0 - M} - 1} a_{mk} \left[\varphi_{mk}(\bar{t}_\iota) - \lambda \int_{A + h * 2^m * k}^{A + h * 2^m * (k+1)} K(\bar{t}_\iota, \tau) \varphi_{Mk}(\tau) d\tau \right],$$

$$B = \sum_{j=1}^{M} \sum_{k=0}^{2^{n_0 - j} - 1} d_{jk} \left[\psi_{jk}(\bar{t}_\iota) - \lambda \int_{A + h * 2^m * k}^{A + h * 2^m * (k+1)} K(\bar{t}_\iota, \tau) \psi_{jk}(\tau) d\tau \right],$$

$$A + B = f\ (\bar{t}_\iota),$$

$$i = 0, 1, \cdots, N - 1;$$

After the coefficients are found from the system of linear algebraic equationsa_{mk} ,$k = 0, 1, \cdots, 2^{n_0 - m} - 1$ and $d_{jk}, j = 1, 2 \ldots M, k = 0, 1, \cdots, 2^{n_0 - j} - 1$,, an approximate solution of x*(t) is constructed.

5.2 The solution of the Fredholm integral equation of the 2nd kind using spline approximations of the zero and first degrees

While Haar wavelets have been in use since 1909, the results on the solution of the Volterra integral equations were published earlier than 1909.

Wavelets have only recently been used to solve integral equations. For example, the authors of paper [1] presented the results of using the Haar wavelets to solve the Fredholm integral equation of the second kind.

In this paper, we will consider the construction of spline approximations of the degree zero. In addition, we will compare the results of using spline approximations of the zero and first degrees for solving the Fredholm integral equation of the second kind. Next, we will compare the results of applying spline approximations of the zero and first degrees for solving the Fredholm integral equation of the first kind. The results obtained using these splines are compared with the results of applying the Haar wavelets.

5.2.1 Theories About Splines

Solomon Grigoryevich Mikhlin, who was a professor at St. Petersburg University developed a coherent theory for constructing Hermitian-type local splines in his work "Variational grid approximation". The main idea was that the approximation is constructed separately on each grid interval as a sum of products of basis splines of non-zero level, and the values of the function (or derivatives of the function up to order α) at grid nodes. In order to construct the basis spline in the very beginning we set the support of the basis spline. After that, the basis splines are found by solving a system of linear algebraic equations. This system is called the approximation relations. The simplest approximations are obtained only when using the values of the function at the grid nodes and basis splines of the zero level. Let the grid nodes $\{x_j\}$ be given on the interval $[a, b]$.

When using only the values of the function at the grid nodes, we construct the approximation in the form

$$\tilde{u}(x) = \sum_j u_j \, \omega_j(x) \, , \quad x \in [x_j, x_{j+1}]$$

Thus, we find the basis functions by solving the system of equations

$$u(x) - \tilde{u}(x) = 0, u = 1, \dots, x^m.$$

The number $m + 1$ is called the order of approximation.

5.2.2 Splines of the zero degree

Consider the case of using only one basis function. We set the support of the basis spline as follows: $supp\ \omega_j = [x_j, x_{j+1}]$.

In this simplest case, we have the following expression for the basis function

$$\omega_j(x) = 1, x \in [x_j, x_{j+1})$$

$$\omega_j(x) = 0, x \notin [x_j, x_{j+1})$$

The graph of this basis function ω_j when $[x_j, x_{j+1}) = [0,1)$ is shown in Fig.3.

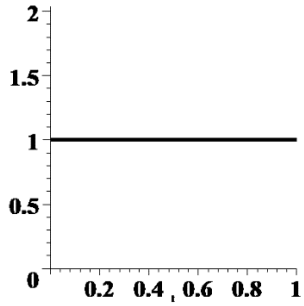

Fig.3. The plot of the basis function ω_j

Obviously, the approximation using these splines is discontinuous. Let the grid of nodes be an equidistant set of nodes, hence it is such that $h = x_{j+1} - x_j$.

In this case, it is easy to obtain an estimate of the approximation error on the interval $[x_j, x_{j+1})$:

$$|u(x) - \tilde{u}(x)| \le h \frac{\sup\limits_{[x_j, x_{j+1})} |u'|}{1!}$$

Note that these splines can be used, for example, to approximate the Runge function

$\frac{1}{1+25\,x^2}$.

Fig. 4 shows a plot of the Runge function approximation error for 20 interpolation nodes on the interval [-1,1]. Fig. 5 shows a plot of the Runge function approximation error for 64 interpolation nodes on the interval [-1,1]. Fig. 6 shows a plot of the Runge function approximation error for 256 interpolation nodes on the interval [-1,1].

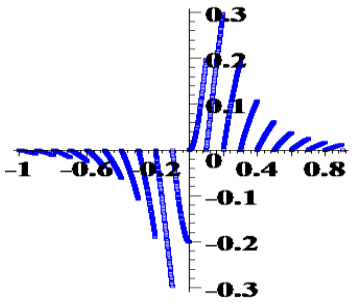

Fig.4. The plot of Runge function approximation error at 20 interpolation nodes

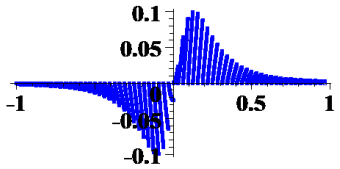

Fig.5. The plot of Runge function approximation error at 64 interpolation nodes

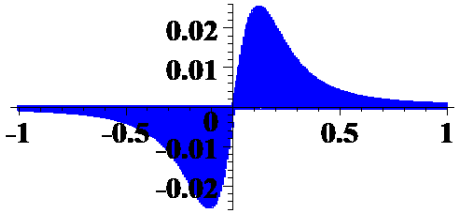

Fig.6. The plot of Runge function approximation error at 256 interpolation nodes

5.2.3 Splines of the first degree

Now we set the support of the basis spline as follows: $supp\ \omega_j = [x_{j-1}, x_{j+1}]$.

On the interval $[x_j, x_{j+1}]$ we approximate the function u by the following expression:

$$\tilde{u}(x) = u(x_j)\omega_j(x) + u(x_{j+1})\omega_{j+1}(x), x \in [x_j, x_{j+1}]$$

where

$$\omega_j(x) = \frac{x - x_{j+1}}{x_j - x_{j+1}} \qquad x \in [x_j, x_{j+1}],$$

$$\omega_j(x) = \frac{x - x_{j-1}}{x_j - x_{j-1}} \qquad x \in [x_{j-1}, x_j],$$

and ω_{j+1} is expressed as:

$$\omega_{j+1}(x) = \frac{x - x_j}{x_{j+1} - x_j} \qquad x \in [x_j, x_{j+1}]$$

The plot of a piecewise linear function ω_j is given in the Fig. 7.

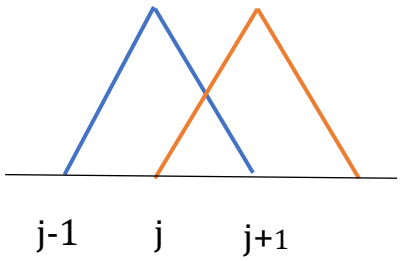

Fig.7. The plot of the basis function ω_j

Obviously, the approximation using these splines is continuous. Let the grid nodes $\{x_j\}$ be given on the interval $[a, b]$, $h = x_{j+1} - x_j$,

In the case of the splines of the first degree, it is easy to obtain an estimate of the approximation error on the interval $[x_j, x_{j+1}]$:

$$|u(x) - \tilde{u}(x)| \leq h^2 \frac{\max\limits_{[x_j, x_{j+1}]} |u''|}{8}$$

Thus we call these splines as splines of the second order of approximation.

5.2.4 The solution of the integral equation with the splines of the zero degree

Consider the solution of the Fredholm integral equation of the second kind

$$u(x) - \int_{\alpha}^{\beta} \mathrm{K}(x, s) u(s)\, ds = f(x)$$

On the interval $[\alpha, \beta]$we construct the set of nodes $x_k = a + kh, h = \frac{\beta-\alpha}{n}$, suppose n is an integer.

We have

$$\int_{\alpha}^{\beta} \mathrm{K(x,s)u(s)\,ds} = \sum_{\mathrm{k=0}}^{\mathrm{n-1}} \int_{\mathrm{x_k}}^{\mathrm{x_{k+1}}} \mathrm{K(x,s)u(s)\,ds}$$

On each interval $[\mathrm{x_k}, \mathrm{x_{k+1}}]$ we replace u with $\tilde{u}$,

$$\tilde{u} = u_k \omega_k(x)$$

where $\omega_k(x)$ is the local spline of degree zero.

Now we have

$$u(x) - \sum_{\mathrm{k=0}}^{\mathrm{n-1}} \int_{\mathrm{x_k}}^{\mathrm{x_{k+1}}} \mathrm{K}(x,s) u_k \omega_{\mathrm{k}}(\mathrm{s})\, ds = f(x)$$

From here we get

$$u(x) - \sum_{\mathrm{k=1}}^{\mathrm{n-1}} u_k A_k(x) = \mathrm{f(x)},$$

where

$$A_k(x) = \int_{\mathrm{x_k}}^{\mathrm{x_{k+1}}} \mathrm{K(x,s)}\omega_{\mathrm{k}}(\mathrm{s})\,\mathrm{ds}.$$

Finally, we take $x_i$instead of *x* and solve the system of equations

$$u_i - \sum_{k=0}^{n-1} u_k \tilde{A}_k(x_i) = f(x_i), i = 0,1,2,\cdots,n-1\,.$$

6 Numerical experiment and conclusion

As an example, we choose the model integral equation from (Е.С.Тарасова, Д.ВТарасов, Метод вейвлет-коллокаций решения интегрального уравнения Фредгольма второго рода, Актуальные вопросы естествознания, Вестник Пензенского государственного университета, 3(7) 2014)

$$u(x) - \frac{1}{10}\int_0^{\frac{\pi}{2}} (x^2 + t)\, u(t)dt = \sin(x) - \frac{1}{10}(x^2 + 1),$$

$$x \in [0, \frac{\pi}{2}]$$

Using the collocation method and Haar wavelets to solve this equation to obtain the numerical results. The results are shown in the last column of the Table 1 (The program was developed in C++).

In particular, at $N = 32$ the norm of absolute error in $L_2$was 0.012. At $N = 128$ the norm of absolute error in $L_2$was 0.0031.

Table 1 also shows the errors in solving the model integral equation obtained using polynomial splines of zero and first degree.

Table 1. Errors in L_2

N	*Spl L_1*	*Spl L_0*	*Vev haar*
16	*0.059*	*0.020*	*0.025*
32	*0.029*	*0.010*	*0.012*
128	*0.0073*	*0.0025*	*0.0031*

Conclusion 1. Minimal polynomial splines of the 0-th and first degree are quite suitable for solving the Fredholm integral equation of the second kind. The quality of the resulting solution is no worse than when using Haar wavelets.

To calculate the approximate solution by polynomial splines of zero and first degree, a program was developed in MAPLE. The beginning of the program looks like this

K:=unapply(-(X^2+t)/10,X,t):

U:=unapply(sin(X),X):

F:=unapply(U(X)+int(K(X,t)*U(t),t=0..Pi/2.0),X);

$$F := X \to \sin(X) - \frac{1}{10}X^2 - 0.100000000000000$$

n:=32;h:=Pi/2./(n):

To solve the system of equations, we use the solve library program. The Gaussian method can be used. We build graphs using POINTPLOT.

The error of the solution when $n = 16$ is given in Fig.6.

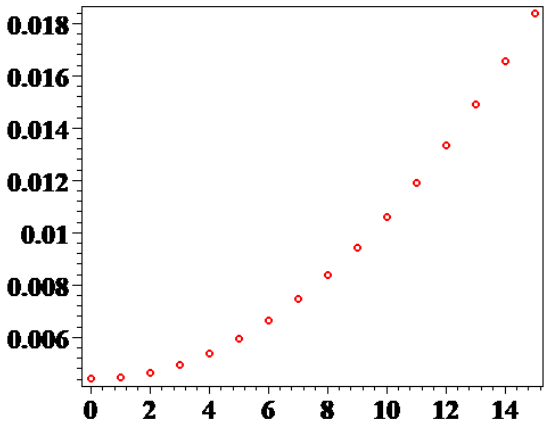

Fig.8. The error of the solution ($h := 0.098174770424681038701957 59$)

At 32 nodes, the graph of the solution error has the form shown in Fig 7. Fig.8. shows the plot of the error of the solution by splines of zero degree at 128 nodes.

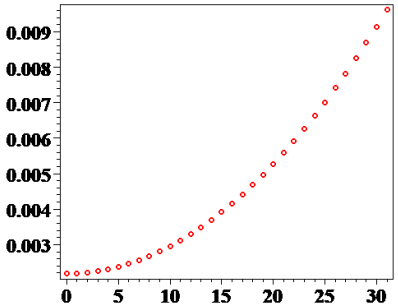

Fig.9. The plot of the error of the solution by splines of zero degree at 32 nodes

($h := 0.049087385212340519350978 80$)

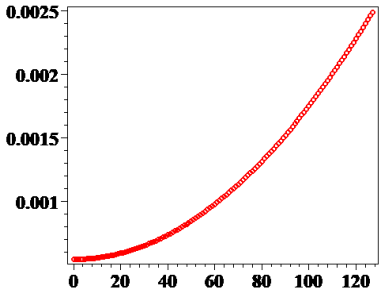

Fig.10. The plot of the error of the solution by splines of zero degree at 128 nodes

($h := 0.012271846303085129837744 70$)

Now Fig.11. shows of the error of the solution by splines of the first degree at 16 nodes ($h := 0.000388254498415$)

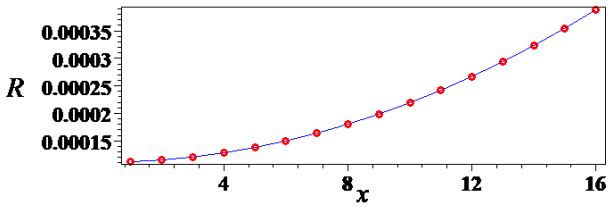

Fig.11. The plot of the error of the solution by splines of the first degree at 16 nodes

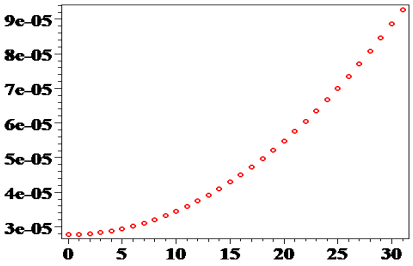

Fig.12. The plot of the solution error with the first-degree splines at 32 nodes .The maximum deviation in absolute value is 0.000088656955789

Table 2. Errors in the first-degree spline and the zero-degree splines

N	*Spl 0*	*Spl 1*
16	*0.09817*	*0.0003883*
32	*0.04909*	*0.00008665*
128	*0.01227*	*0.00001268*

Conclusion 2. The error of the first degree splines is only about one-tenth of the level 0 spline.Minimal polynomial splines of the first degree are more suitable for solving the Fredholm integral equation of the second kind in a small range.

Example 2. As a model example, we choose the model integral equation of the first kind

$$-\frac{1}{10}\int_0^{\frac{\pi}{2}}(x^2+t)\,u(t)dt = \sin(x) - \frac{1}{10}(x^2+1),$$

$$x \in [0, \frac{\pi}{2}]$$

We get the system of equations

$$MU = F$$

after applying splines of the zero degree:

$$S := \{u_0 = -40.67219289,\ u_1 = 28.44169962,\ u_2 = 48.55073318,\ u_3 = 14.22325369,$$
$$u_4 = -22.12511724,\ u_5 = -24.85845202,\ u_6 = 5.546501340,\ u_7 = -14.41728649,$$
$$u_8 = -12.11465808,\ u_9 = 1.029858521,\ u_{10} = 1.008970221,\ u_{11} = 24.92387115,$$
$$u_{12} = -2.105225132,\ u_{13} = 2.347598532,\ u_{14} = -0.230258026\}$$

The error of the solution given in Fig.11.

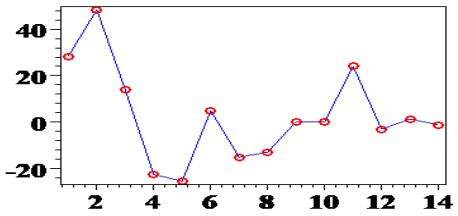

Fig.11. The plot of the solution error with the first-degree splines at 16 nodes without regularization

After Tikhonov's regularization

$$(M^*M + \alpha E)U = M^*F$$

we get the error solution given in Fig.12.

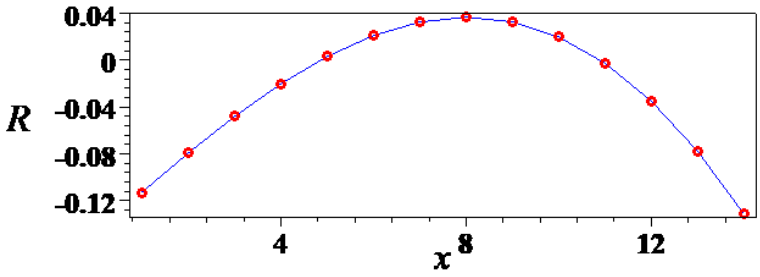

Fig.12. The plot of the solution error with the first-degree splines at 16 nodes after Tikhonov's regularization

Conclusion 3.

Minimal polynomial splines of the first degree is quite suitable for solving the Fredholm integral equation of the first kind after Tikhonov's regularization, the first degree spline has a good performance.

Conclusion

This paper provides a historical view of theories about wavelets. After that,it also provide the formula to construct a numercial experiment to the solution of integral equations. within the comparison with different wavelets, the result shows a small acceptable error gap.The use of wavelets to solve integral equations by collocation method has shown good efficiency. In addition, the use of a certain type of wavelet as a basis function makes it possible to obtain an integral in the form of a numerical or analytical calculation. This feature can have a positive impact in solving singular and hyperspherical integral equations. Therefore, the wavelet collocation method for calculating the numerical solutions of mathematical problems can open up new features in the construction of stable algorithms.

References

[1] Добеши И. Десять лекций по вейвлетам. М.-И. 2004. 464 с.

[2] Skopina M. Multiresolution analysis of periodic functions// East Journal on Approximations. 1997. Vol.3, №2. P.614-627.

[3] Новиков И.Я., Стечкин С.Б. Основы теории всплесков// Успехи математич. наук. 1998. Т.53, № 6. С.53-128.

[4] Петухов А.П. Введение в теорию базисов всплесков. СПб., 1999. 132 с.

[5] Чуи К. Введение в вэйвлеты. М. 2001. 412 с.

[6] Малла С. Вэйвлеты в обработке сигналов. М. 2005. 671 с.

[7] Daubechies I., Guskov I., Schr¨oder P., Sweldens W. Wavelets on Irregular Point Sets//Phil.Trans.: Math., Physical,Engng.Sci., 357(1999). P. 2397-2413.

[8] Daubechies I., Guskov I., Sweldens W. Commutation for Irregular Subdivision//Const. Approx., 17(4),(2001). P.479-514.

[9] Aldroubi A., Sun Q., Tang W.-S., Non-uniform average sampling and reconstruction in multiply generated shift-invariant spaces// Constr. Approx., 20 (2004). P. 173–189.

[10] Aldroubi A., Cabrelli C., Molter U. Wavelets on irregular grids with arbitrary dilation matrices, and frame atoms for L 2 (R d). Preprint. Date: March 30, 2004. http://atlas.math.vanderbilt.edu/∼aldroubi/IW.ps

[11] Стечкин С.Б., Субботин Ю.Н. Сплайны в вычислительной математике. М., 1976. 248 с.

[12] Завьялов Ю.С., Квасов Б.И., Мирошниченко В.Л. Методы сплайнфункций. М., 1980. 352 с.

[13] Schumaker L.L. Spline Functions. Basic Theory. Waley Interscience. New York. 1981. 548 p.

[14] Малоземов В.Н., Певный А.Б. Полиномиальные сплайны. Л.,1986. 120 с.

[15] Buchwald B., M¨uhlbach G. Construction of B-splines for generalized spline spaces from local ECT-systems// Journal of Computational and Applied Mathematics 159 (2003). P. 249-267.

[16] M¨uhlbach G. ECT-B-splines defined by generalized divided differences// Journal of Computational and Applied Mathematics 187 (2006). P. 96-122. 48

[17] Goel J.J. Construction of basis functions for numerical utilization of Ritz's method// Numer. Math. 1968. Vol. 12. P.435-447.

[18] Strang G., Fix G. Fourier analysis of the finite element method in Ritz-Galerkin theory// Stud. Appl. Math. 1969. Vol.48, №3. P. 265-273.

[19] Михлин С.Г. Вариационно-сеточная аппроксимация// Зап. науч. семинаров ЛОМИ АН СССР. 1974. Т.48. С. 32-188.

[20] Демьянович Ю.К., Михлин С.Г. О сеточной аппроксимации функций соболевских пространств// Зап. науч. семинаров ЛОМИ АН СССР. 1973. Т.35. С. 6-11.

[21] Демьянович Ю.К. Локальная аппроксимация на многообразии и минимальные сплайны. СПб., 1994. 356 с.

[22] Бурова И.Г., Демьянович Ю.К. Теория минимальных сплайнов. СПб., 2000. 316 с.

[23] Демьянович Ю.К. Всплески & минимальные сплайны. СПб., 2003. 200 с.

[24] Демьянович Ю.К. О вложенности пространств минимальных сплайнов// Ж. выч. мат. и мат. физ. 2000. Т.40. № 7. С. 1012-1029.

[25] Демьянович Ю.К. Гладкость пространств сплайнов и всплесковые разложения// Доклады РАН. 2005. Т.401, № 4. С. 1-4.

[26] Демьянович Ю.К., Иванцова О.Н. Гладкость пространств сплайнов третьего порядка. Сб. Математические модели. Теория и приложения. Вып.7. СПб.: ВВМ, 2006. С. 58-64.

[27]Манжиров, А. В. Справочник по интегральным уравнениям: методы решения / А. В. Манжиров, А. Д. Полянин. – М. : Факториал Прес, 2000. – 384 с.

[28]Beylkin, G. Fast wavelet transforms and numerical algorithms / G. Beylkin, R. Coifman, V. Rochlin // Comm. Pure. Appl. Math. – 1991. – V. 44. – P. 141–183.

[29]Рогова, Н. В. Методы вейвлет-анализа численного решения одномерных задач электродинамики : автореф. дис. … канд. физ.-мат. наук / Рогова Н. В. – Воронеж, 2008. – 16 с.

[30]Бойков, И. В. Приближенные методы решения сингулярных интегральных уравнений / И. В. Бойков. – Пенза : Изд-во Пенз. гос. ун-та, 2004. – 316 с.

[31]Бойков, И. В. Приближенные методы вычисления интегралов Адамара и решения гиперсингу- лярных интегральных уравнений / И. В. Бойков, Н. Ф. Добрынина, Л. Н. Домнин. – Пенза : Изд-во Пенз. ГТУ, 1996. – 188 с.

[32]Бойков, И. В. Применение гиперсингулярных интегральных уравнений к численному модели-рованию электрического вибратора / И. В. Бойков, Д. В. Тарасов // Известия высших учебных
заведений. Поволжский регион. Технические науки. – 2008. – № 4. – С. 94–106.

[33] Бойков, И. В. Приближенное решение некоторых классов гиперсингулярных интегральных уравнений / И. В. Бойков, Б. М. Стасюк, Д. В.

Тарасов // Известия высших учебных заведений. Поволжский регион. Физико-математические науки. – 2009. – № 1 (9). – С. 100–112.

[34] Яковлев, А. Н. Введение в вейвлет-преобразования : учеб. пособие / А. Н. Яковлев. – Новосибирск : Изд-во НГТУ, 2003. – 104 с.

[35]Воробьев, В. И. Теория и практика вейвлет-преобразования / В. И. Воробьев, В. Г. Грибунин. – СПб. : Изд-во ВУС, 1999. – 208 с.

[36] S. Mallat, A Wavelet Tour of Signal Processing, Academic Press, 1999. DOI: 10.2118/96553-MS.

[37]Novikov I.Ya., Protasov V.Yu., Skopina M.A. Wavelet Theory. AMS, Translations Mathematical Monographs, V. 239 (2011). 506 pp. ISBN 978-0-8218-4984-2.

[38]Yu. K. Dem'yanovich, "Wavelet decompositions on nonuni form grids" Am. Math. Soc. Transl. Ser. 2 222, 23–42 (2008). DOI: 10.1007/s10958-009-9752-0

[39]Yu. K. Dem'yanovich, "Wavelets on a mani
fold," Dokl. Math. 79, No. 1, 21–24 (2009).
DOI:10.1134/S1064562409010074

[40] Yu. K. Dem'yanovich and A.Yu.Ponomareva. "Adaptive Spline-Wavelet Processing of a Discrete Flow", J. Math. Sci., New York 210, No 4, pp.371-390 (2015). DOI: 10.1007/s10958-015-2571-6

[41] Yu.K.Dem'yanovich, A.S.Ponomarev. "On realization of the Spline-Wavelet Decomposition of the First Order", J. of Math. Sci. Vol. 224, No.6, pp.833-860 (2017). DOI: 10.1007/s10958-017-3454-9.

[42]S.G. Michlin, Approximation auf dem Kubischen Gitter, Berlin, 1970. ISBN-s: 3034854994 / 9783034854993.

[43]J.N. Reddy, An Introduction to the Finite Element Method (Third ed.).McGraw-Hill. 2006. ISBN 0-07-051355-4[44]O.C. Zienkiewicz, R.L. Taylor, J.Z. Zhu, The Finite Element Method: Its Basis and Fundamentals (Sixth ed.). Butterworth-Heinemann. 2005. ISBN 0-750-6320-0.

[45] Ivo Babuska, Uday Banerjee, John E. Osborn, "Generalized Finite Element Methods: Main Ideas, Results, and Perspective", International Journal of Computational Methods 1 (1), 2004, pp.67-103. DOI: 10.1142/S0219876204000083.

[46]G. R. Liu, K. Y. Dai, T. T. Nguyen, "A smoothed fifinite element method for mechanics problems", Comput. Mech. 39, 2007, pp.859 -– 877. DOI: 10.1007/s00466-006-0075-4

[47] G. R. Liu, T. T. Nguyen, K. Y. Dai and K. Y. Lam, "Theoretical aspects of the smoothed fifinite element method (SFEM)", Int. J. Numer. Meth. Engng. 71, 2007, pp.902- 930. DOI: 10.1002/nme.1968.

[48] G.R. Liu, Smoothed Finite Element Methods, CRC Press, 2010. ISBN 9781439820278.

[49] T. Nguyen-Thoi, G. R. Liu and H. Nguyen-Xuan, "An nsided polygonal edge-based smoothed fifinite element method (nES-FEM) for solid mechanics", Int. J. Numer. Meth. Biomed. Engng. 2010, (www.interscience.wiley.com). DOI: 10.1002/cnm.1375

[50] Vahid Shobeiri, "Structural Topology Optimization Based on the Smoothed Finite Element Method", Latin American Journal of Solids and Structures, 13, 2016, pp.378-390. DOI: 10.1590/1679-78252243.

[51] Е.С.Тарасова, Д.ВТарасов, Метод вейвлет-коллокаций решения интегрального уравнения Фредгольма второго рода, Актуальные вопросы естествознания, Вестник Пензенского государственного университета, 3(7) 2014)